Available online at www.sciencedirect.com

ScienceDirect

Procedia CIRP 14 (2014) 535 – 540

www.elsevier.com/locate/procedia

6th CIRP International Conference on High Performance Cutting, HPC2014

Finite element model to calculate the thermal expansions of the tool and the workpiece in dry turning

S. Schindler[a*], M. Zimmermann[b], J.C. Aurich[b], P. Steinmann[a]

[a]*University of Erlangen Nuremberg, Chair of Applied Mechanics, Egerlandstr. 5, 91058 Erlangen,* Germany
[b]*University of Kaiserslautern, Institute for Manufacturing Technology and Production Systems, Gottlieb-Daimler-Str., 67663 Kaiserslautern*, Germany

* Corresponding author. Tel.: +49-9131-8528506 ; fax: +49-9131-8528503. *E-mail address:* Stefan.Schindler@ltm.uni-erlangen.de

Abstract

Dry cutting is an important issue with regard to the economy and ecology of machining. The absence of the cutting fluid reduces both the costs for machining and the risk of ecological hazards. However, the missing convection through the cutting fluid increases the temperatures of the workpiece and the tool, and thus their thermal expansions. As a result, remarkable deviations from the nominal workpiece geometry occur. To enhance the accuracy of machining when dry turning, the thermal expansions of the tool and the workpiece can be calculated prior to actual turning using finite element (FE) models in order to adapt the nominal depth of cut accordingly. Therefore, an experimentally validated (using aluminum as the workpiece material) FE model is presented. The FE model inputs the heat flux into the tool and the workpiece as boundary conditions. The heat flux is applied locally and temporally discretized to the workpiece and the tool in the chip formation area. Their thermal expansions can thus be calculated in terms of the cutting condition used and the tool position, whereby process planning regarding the machining accuracy is facilitated.

Selection and peer-review under responsibility of the International Scientific Committee of the 6th CIRP International Conference on High Performance Cutting

Keywords: Thermal expansion; Dry turning; Finite element;

1. Introduction

In machining, mechanical work is dissipated into thermal energy because of the plastic deformation of the workpiece material during the chip formation and the friction between the tool and the workpiece material. For wet machining a significant portion of the generated heat is absorbed by the cutting fluid. The missing cutting fluid in dry machining causes thus remarkably greater thermal loads on the workpiece and the tool [1, 2]. These thermal loads lead to expansions, which increase the actual depth of cut accordingly. As a result, the accuracy of machining is decreased [3-5].

To enhance the accuracy of machining when dry turning, the cutting condition used can be firstly defined with regard to low thermal loads on the workpiece and the tool. Moreover determining the thermal expansions of the tool and the workpiece allows a further optimization of the machining accuracy through accordingly adapted depths of cut. For this purpose, experimental investigations were frequently used. In order to prevent cost and time-intensive experimental investigations, the effort to develop finite element models allowing for the prediction of the actual workpiece geometry after machining regarding the cutting condition used increases in recent years. In [6] a FE model to predict the actual workpiece geometry after turning, considering the material removal and the thermal expansion of the workpiece, is described. The heat flux into the workpiece is experimentally determined and used as boundary condition. FE models of the chip formation process calculating the heat flux into the workpiece are presented in [7] and [8] for drilling. An approach using a dexel model to perform the material removal and a FE model to calculate the thermal effects on the machining accuracy during milling is outlined in [9]. A comparison of several effects on the accuracy of machining when hard turning is shown in [10]. Thermally induced deformations of the tool and the workpiece were revealed as significant.

Selection and peer-review under responsibility of the International Scientific Committee of the 6th CIRP International Conference on High Performance Cutting
doi:10.1016/j.procir.2014.03.087

In this paper, FE models of the system tool-tool holder and the workpiece are outlined. These FE models calculate the thermal expansion of the respective components with regard to the cutting condition used and the position of the tool along the feed travel. The required heat fluxes were experimentally determined. Thermally induced deformations of the system tool-tool holder and the workpiece during turning can thus be compensated through accordingly adapted depths of cut. This allows enhancing the accuracy of machining in actual turning.

2. Experimental Setup

Dry cutting investigations were carried out on a CNC lathe using the aluminum alloy Al2024 as the workpiece material. The cutting speed v_c was varied from 100 m/min to 300 m/min, the feed f from 0.1 mm/rev. to 0.3 mm/rev., and the depth of cut a_p ranged from 0.5 mm to 1.5 mm. The workpieces (geometry, Fig. 2) were fixed in a chuck and supported by the center of the tailstock. Thus, the deflection of the workpiece through the forces is decreased.

Polycrystalline diamond (PCD) was used as the cutting material. The PCD was brazed on a cemented carbide substrate. The tool possesses the following geometry (DCMT 11T304): clearance angle 7°, rake angle 0°, tool cutting edge inclination 0°, tool cutting edge angle 93°. In order to prevent appreciable influence of wear on the results, new tools were used prior the formation of significant wear (width of flank wear land << 100 µm).

Four characteristic values were experimentally determined to be able to model thermal effects on the accuracy of machining: the temperature distribution of the tool, the tool holder, and the workpiece, the forces, and the diameter of the workpiece after dry turning. To evaluate the temperature of the tool and the tool holder both thermocouples (Typ K, wire diameter 0.5 mm) and a commercial thermal imaging camera (Flir SC7600) were used. The thermal imaging camera operates with wavelengths from 1.5 µm to 5.1 µm (infrared). The positions of the five thermocouples are depicted in Fig. 1. The temperature inside the tool holder was detected at three positions. Two thermocouples (MP_t2 and MP_t4) were positioned behind the contact area with the tool in different distances to the contact area. An additional thermocouple is positioned directly below the dynamometer (MP_t5).

Two thermocouples were used to determine the temperature of the tool at the contact area between the tool holder and the tool (MP_t1 and MP_t3, Fig. 1). These temperatures are lower than the temperatures of the tool on the rake face. By using a thermal imaging camera, the temperature of the tool on the rake face and the tool holder surface can be measured. These temperatures were evaluated immediately after the last tool engagement. During the tool engagement, thermal imaging of the rake face and the tool holder surface is strongly affected by the chips, and thus not appropriate. The coefficients of emission e of the cutting material (PCD, $e_1 = 0.81$), the cemented carbide ($e_2 = 0.68$) and the tool holder ($e_3 = 0.95$) were determined in preliminary investigations. The presented images (in section 4) are the result of the superposition of different plots recorded by means of the thermal imaging camera. Each of these plots was evaluated using the determined coefficient of emission for the respective material. Multiple aperture times of the thermal imaging camera were used simultaneously in order to detect the present temperature range.

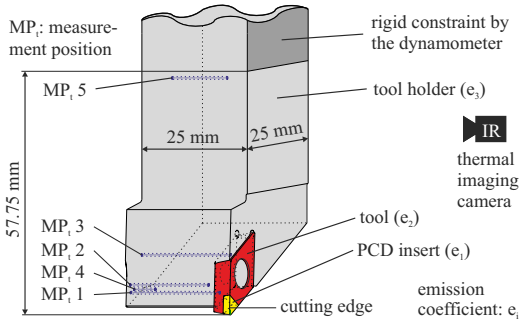

Fig. 1. Experimental setup of the cutting tool.

The workpiece temperature was measured at three positions inside the workpiece using thermocouples (Typ K, wire diameter 1 mm) (Fig. 2). The signals of these thermocouples were collected by means of wireless data acquisition. Preliminary investigations with different thermocouple positions showed that the major temperature gradient is in axial direction, while the temperature gradient in radial direction is low [11]. Thus, the thermocouples for the actual investigations were positioned in different axial positions and centered regarding the radius of the workpiece after machining. The tangential position was homogenously distributed (indicated by the angle of 120° in Fig. 2) to minimize the interaction between the individual thermocouples.

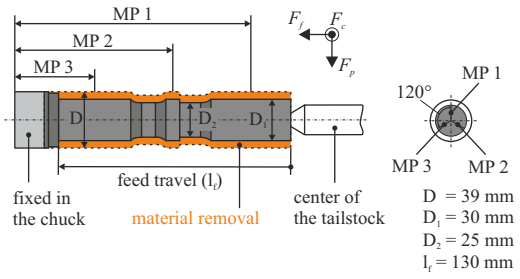

Fig. 2. Experimental setup of the workpiece.

During a specific tool engagement each measurement position and hence each material point undergoes approximately the same temperature increase ΔT when the tool passes the respective position (Fig. 5). As a result, the heat flow into the workpiece $\mathfrak{Q}_{win}$ (for the modeling of the heat input in the FE simulations) due to turning can be calculated from the temperature increase per time of an individual tool engagement Δt:

$$\mathfrak{Q}_{win} = \rho V c \frac{\Delta T}{\Delta t}, \qquad (1)$$

where V is the volume of the workpiece at the respective tool engagement, ρ is the density, and c is the heat capacity. For an individual cutting condition the heat flux into the workpiece is approximately constant at multiple tool engagements, because chip formation does not alter. There are also analytical methods to determine the heat flux into the workpiece, e.g. Shaw [12]. Shaw calculates the heat flux into the workpiece from the chip geometry and the cutting forces. Measuring the chip geometry is often difficult and the method of Shaw is like many others limited to orthogonal cut. In contrast the here described experimental based method is valid for arbitrary turning operations. The measurement of the temperature inside the workpiece seems to be also difficult in particular for turning, but it is anyway necessary to verify the simulated temperature distribution. At the first tool engagement, heat fluxes to the environment (heat convection and heat conduction) can be neglected due to the small temperature difference between the workpiece and the environment. However, when using multiple tool engagements for turning the heat flux to the environment needs to be considered due to the greater temperature of the workpiece. For this purpose the coefficient of heat conduction into the chuck and of heat convection to the ambient air were determined. Radiation is negligible at the present workpiece temperatures.

The forces were measured using a three-component dynamometer. The mean of the cutting force F_c, the feed force F_f and the passive force F_p during the tool engagements was calculated in order to evaluate the forces. The actual diameter of the workpiece after turning was measured at 16 positions along the feed travel by means of a 3D-coordinate measuring system. Each investigation using a specific cutting condition was repeated three times.

3. FE-models of the tool and the workpiece

The FE simulations are performed using a separate model for the workpiece and the tool, respectively. Each of these models calculates the temperature distribution, the related thermal expansion and the deflection due to the forces. Both FE models use the heat flux, the forces, and the coefficients of heat transfer as boundary conditions. These were experimentally determined. The magnitude of the heat flux and the forces are approximately constant for a defined cutting condition at an individual tool engagement. Measuring these loads once allows using them virtually for arbitrary workpiece geometries.

The FE model of the tool consists of the tool and the tool holder (Fig. 3). The tool holder needs to be considered because the evaluation of the experiments showed that the tool holder is subjected to a significant temperature increase during turning. The device used to clamp the tool holder (in this case the dynamometer) possesses, however, no significant temperature increase. Thermo-mechanical material properties are required in the FE model for the tool holder (Aisi4140), the cemented carbide substrate (K10), and the PCD. These are listed in Tab. 1. The mechanical contact between these parts is assumed as rigid, because a relative displacement between these parts should not occur in macroscopic scales. The thermal contact is assumed as ideal.

The heat flux to the tool was applied at the contact area with the workpiece and the chip, respectively, i.e. at a small surface area around the cutting edge that is roughly approximated by the cross-section of undeformed chip (Fig. 3). A pre-processor evaluates the numerical control (NC) code of the lathe in order to subject the heat flux and the forces time-dependent to the tool. For this purpose, the pre-processor determines the time increments in which the tool is engaged.

Table 1. Material properties of the tool, the tool holder and the workpiece.

Material	E [GPa]	ν [-]	ρ [kg/m³]	c [J/kgK]	λ [W/mK]	κ [µm/mK]
PCD	800	0.3	3520	600	520	2.62
K10	650	0.21	14900	200	100	5.0
Aisi4140	220	0.3	7850	450	48	11.5
Al2024	73.1	0.33	2780	875	151	23.2

The heat flux into the tool was determined using an inverse identification. Therefore, an initial heat flux is assumed to calculate the temperature distribution in the tool and the tool holder for a specific cutting condition. These temperature distributions are evaluated at the five measurement positions depicted in Fig. 1. The numerically determined temperatures are afterwards compared with the experimentally measured temperatures. The comparison is performed when the first measurement position undergoes a temperature increase (short time of machining). The global temperature of the tool holder is at that time still low, and thus the heat flux to the environment affecting the experimentally measured temperatures is negligible. Detected differences between simulated and measured temperatures are adjusted using a least squares curve-fitting algorithm. Solving this curve-fitting in least-square sense means in this case, finding the heat flux into the tool q_{tin} (coefficient x in equation 2) that solves the problem:

$$\min_x \left\| F(x,t) - T(t) \right\|_2^2 = \\ = \min_x \sum_i (F(x,t_i) - T(t_i))^2, \tag{2}$$

where the time t is the given input data and the measured temperature $T(t)$ is the observed output. F is a function, in this case the FE simulation that calculates the temperature with regard to the applied heat flux q_{tin} and the time t.

Afterwards a longer time interval of the process is considered. Here the heat flux to the environment is not negligible. At this time, the heat flux into the tool is known due to the preliminary consideration of the short time interval of the process. Consequently, the coefficients of heat transfer (α_{tcv} for convection and α_{tcd} for conduction) are currently the unknown coefficients x in equation (2) and can be determined in the same way as the heat flux into the tool. The curve-fitting algorithm is performed in matlab, which calls the FE simulation as function $F(x,t)$. Separate coefficients of heat convection are determined for the PCD insert, the tool, and the tool holder (Fig 3). Furthermore, a coefficient of heat conduction that determines the heat flux into the dynamometer is ascertained. The experimentally measured

forces are applied time-dependent to the same area on which the heat flux into the tool is applied.

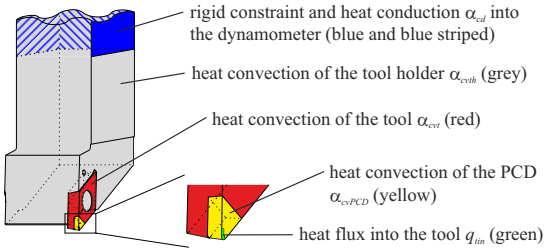

Fig. 3. FE model of the tool and applied boundary conditions.

In a previous publication, the present authors made a first attempt to enhance the accuracy of machining through the simulation of the thermo-elastic deformations of the workpiece [6]. However, it was found that the thermo-elastic deformations of the tool significantly affect the accuracy of machining. Thus, the FE model of the workpiece outlined in detail in [6] is supplemented by the present FE model of the tool. The material properties of the used aluminum alloy Al 2024 are listed in Tab. 1.

The heat flux into the workpiece q_{win} can be assumed as axisymmetric due to the high rotational speed of the workpiece when turning [2]. Experimental turning investigations revealed an insignificant temperature gradient in circumferential direction inside the workpiece [11]. The assumption of an axisymmetric heat flux into the workpiece is thus confirmed. Significant temperature gradients arise locally on the surface layer of the workpiece close to the chip formation area. These temperature gradients are however not important in terms of the overall heating and the dependent thermal expansion of the workpiece and can be neglected for the present model. The forces are not axisymmetric and actually producing alternating stresses. Since the stresses are far below the yield strength of the workpiece material, they can be assumed as static in terms of the rotation of the workpiece. The centrifugal forces of the workpiece are negligible compared to the passive, feed and cutting force. Thus, the rotation of the workpiece can be neglected during the FE simulations. The chuck is assumed as a rigid restraint. The center of the tailstock is considered in the FE model of the workpiece in order to allow for the modeling of the workpiece deflections due to the forces.

The heat flux and the forces are applied on the workpiece in the chip formation area. The NC code defines the location of the tool and hence the location of the chip formation area at each time increment. The developed pre-processor is used to evaluate the tool paths from the NC code.

To facilitate the removal of material the workpiece is meshed according to the respective nominal tool paths by the developed pre-processor. Thus, all element edges in the regions to be machined are either parallel or perpendicular to the tool path. The parallel element edges do not fit the nominal tool path due to the thermal expansion and deflection of the workpiece. The actual tool path hence approximately cuts each element at the middle of the element edges, which are perpendicular to the tool path. Therefore, the element edge length should not exceed the depth of cut. This facilitates the required mesh refinement in order to remove the workpiece material above the nominal tool path. Using an h-adaptive (variation of the element edge lengths and number of elements during remeshing) mesh refinement, each element to be cut by the tool path is subdivided into eight new elements. The newly defined nodes are positioned exactly on the interception point of the nominal tool path and the element edge. Consequently, the new element edges fit exactly the nominal tool path. The removal of material is performed by element deactivation, whereby all elements to be removed are above the nominal tool path. As a result, the actual workpiece diameter after turning can be calculated. Each element is first refined and afterwards deactivated when the tool passes the respective position. Remeshing and deactivation times are controlled by the evaluated NC code.

The material removal at the model of the workpiece is actually influenced by the thermal expansion and deflection of the tool, which change the depth of cut. Considering this change of the depth of cut in the tool path used in the model of the workpiece would increase its accuracy. This effect is not considered in the present model of the workpiece, since it accounts only for approximately 3% of the used nominal depths of cut. For cutting processes with greater changes of the depth of cut, a consideration of this interdependency could be reasonable. For this purpose, the tool path used in the model of the workpiece needs to be modified by the respective deformation of the tool. The generated heat and thus the heat flows into the workpiece and the tool are also influenced by the change of the depth of cut due to the tool and workpiece deformation. This is also not considered for the investigated turning process, because the overall change in the depth of cut due to the thermo-mechanically induced deformations is less than 5%.

The surface of the workpiece and consequently the surface to be considered for heat convection to the environment are continuously adapted according to the removed material. Thermal and elastic properties are used to describe the behavior of the material of the workpiece.

4. Results

In this section experimental and numerical results are presented for one cutting condition: v_c = 300 m/min, f = 0.1 mm/rev., and a_p = 0.9 mm. As a result of the considered depth of cut, five tool engagements are required in order to manufacture the targeted workpiece geometry.

Simulated and measured temperature distributions in the tool and the tool holder are depicted in Fig. 4. The inverse identification of the heat flux into the tool revealed a heat flow of $\mathfrak{Q}_{tin}$ = 35.5 W. The coefficients of heat convection α_{cv} were determined to 50 W/m²K for the PCD insert and 100 W/m²K for the cemented carbide substrate and the tool holder. The coefficient of heat conduction α_{cd} into the dynamometer was determined to 1100 W/m²K. Both simulated and measured tool and tool holder temperatures show a remarkable temperature increase when the time of machining rises. However, the tool is subjected to a considerably greater

temperature change at the initial stages of the respective tool engagements (Fig. 4). The temperature of the tool decreases rapidly when the tool is not in engagement. This confirms the significance of the considered heat convection and heat conduction to the environment; the simulation reveals a maximum heat flow to the environment of 24.4 W, which is 2/3 of the heat flow into the tool. The temperatures of the tool holder at MP_t4 and MP_t5 increase continuously. This can be attributed to the time delayed heating of the tool holder through the heat conduction from the tool (heated only during turning) to the tool holder.

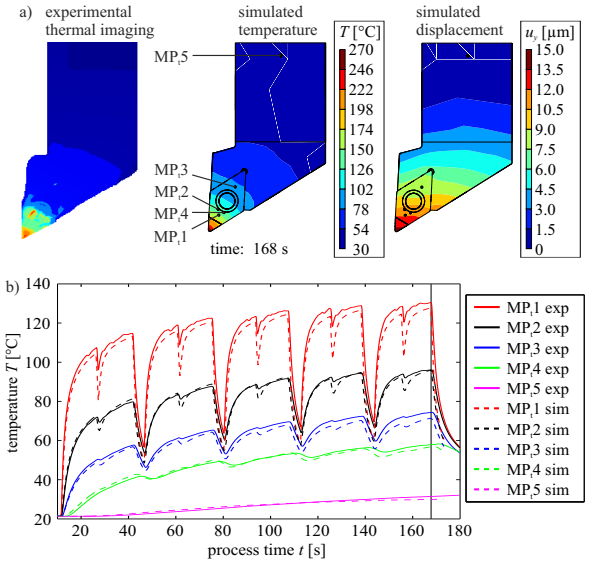

Fig. 4. Temperature distribution and thermal expansion of the tool.

The simulated temperatures at the five measurement positions fit the measured values particularly when the tool is in engagement (Fig. 4b) and under consideration of the standard deviation of the experiment of 8%. When the tool is not in engagement, the calculated temperatures differ slightly from the measured ones. This is mainly caused by the determination of the heat flux to the environment, which is generally an approximation. In practice, this heat flux is influenced by several effects, such as: a non-constant ambient temperature, temperature-dependent coefficients of heat convection and non-constant velocities of the ambient air. These effects are difficult to determine; they are neglected in the present simulation. However, the temperatures during the tool engagements affect the accuracy of machining. These are appropriately predicted. Consequently, the calculated thermal expansion of the system tool-tool holder is adequate. The displacement of the system tool-tool holder in direction of the depth of cut, i.e. the increase of the nominal depth of cut, rises from approximately 11 µm at the initial stages to 15 µm at the final stages of the last tool engagement. The resultant deviation from the nominal workpiece diameter varies thus from 22 µm to 30 µm (Fig. 6). The deflection of the tool due to the forces was also calculated. The cutting condition used reveals a small passive force of 12 N. As a result, the displacement in the direction of the depth of cut is also small (approximately 1 µm). Such displacements decrease the actual depth of cut.

The temperature distribution in the workpiece is illustrated in Fig. 5. The simulated values fit the measured ones particularly at the first tool engagement. The use of multiple tool engagements leads to a deviation of up to 10%, which is the sum of several inaccuracies. Note that the standard deviation of the experiment is already 5%. Such inaccuracies are the approximation of the heat flow into the workpiece (which was determined to 95 W) and of the heat flux to the environment (coefficient of heat convection α_{cv} = 80 W/m²K; coefficient of heat conduction into the chuck α_{cd} = 1100 W/m²K). As a result of the heat flow to the chuck and the unmachined part of the workpiece (to clamp the workpiece) the workpiece temperature at MP3 is lower compared to the temperatures at MP1 and MP2. After the first tool pass only a small temperature decrease was observed at each MP due to the low temperature difference and thus low heat flow to the environment. In contrast, significant temperature decreases were observed at each MP after the last tool pass due to the remarkably increased temperature difference to the environment. This confirms the significance of the heat convection and heat conduction to the environment on the workpiece temperature; the simulation reveals a maximum heat flow to the environment of 46.9 W, which is 1/2 of the heat flow into the workpiece.

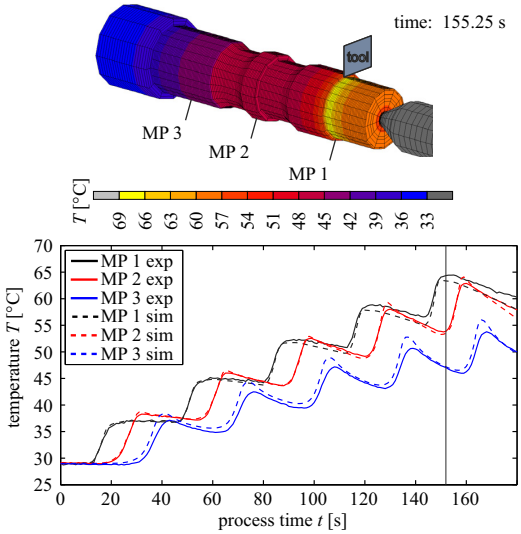

Fig. 5. Temperature distribution of the workpiece.

The calculated thermal expansion of the workpiece (with regard to the diameter of the workpiece) and consequently the deviation from the nominal diameter ranges from approximately 15 µm to 25 µm (Fig. 6). The thermal expansion of a specific object is generally determined by its coefficient of thermal expansion, the dimensions, and the present temperature increase. The smaller nominal diameters of the workpiece (indicated by the two green marked areas in Fig. 6) possess minor thermal expansions than the adjacent

areas of greater nominal diameter. The calculated thermal expansions of the workpiece material are approximately in accordance with the determined temperature distribution in the workpiece. The higher the temperatures at a particular diameter, the greater are the thermal expansions. The present tool temperatures are remarkably greater than the temperatures in the workpiece. Contrary to that, the coefficient of thermal expansion of the workpiece material is approximately five times greater than the coefficient of thermal expansion of the tool and tool holder materials. Nevertheless the diameter deviation caused by the thermal expansion of the tool is larger than the deviations caused by the thermal expansion of the workpiece for the current process. Mechanically induced deflections of the workpiece due to the thrust force account for approximately 1 µm. Thermal effects increase contrary to mechanically induced deflections the actual depth of cut. The actual dimensions of the workpiece are undersized. Thus, the thermal expansions of the tool and the workpiece are predominant for the accuracy of machining when dry turning at the present workpiece.

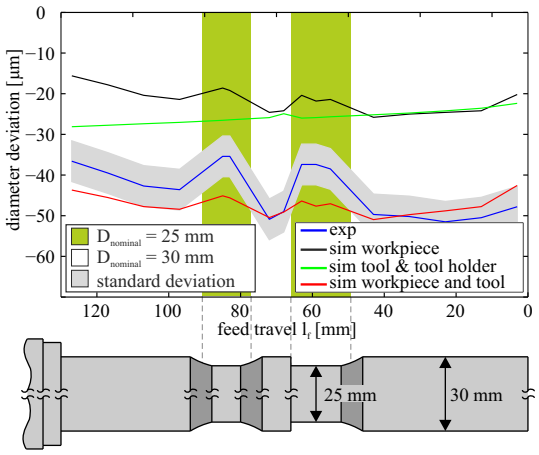

Fig. 6. Diameter deviation.

The accuracy of machining is generally affected by multiple factors of influence. The thermal expansion and deflection of both the workpiece and the tool are considered in the presented FE models. Moreover, effects such as: the thermal expansion of the structure of the machine tool, the displacement of the cutting edge due to the flank wear, and the positioning accuracy of the machine tool influence the actual depth of cut. These effects are not considered in the presented FE models, because separate FE models are required for this purpose. They are however partly considered in the calculated standard deviation for the experimentally detected deviation from the nominal workpiece diameter. Fig. 6 reveals furthermore that the deformations of the tool and the workpiece account for the greatest inaccuracies when dry turning in the present setup. The difference between experimental and numerical results in terms of the determined diameter deviation when turning at varying nominal diameters might be caused by the machine tool (e.g. the interpolation technique in order to manufacture the radius contour, Fig. 2).

5. Conclusion

The described FE models allow calculating the diameter deviation of the workpiece due to the thermal expansion and deflection of the workpiece and the system tool-tool holder. The FE models use the heat fluxes into the workpiece and the tool, the heat fluxes to the environment, and the forces as boundary conditions. These boundary conditions were determined by appropriate experimentally based methods. The calculated temperature distributions in the tool, tool holder and the workpiece match the experimentally measured temperatures. It can thus be concluded, that the predicted thermal expansions are adequate. A comparison of the calculated thermal expansions of the tool and the workpiece with the overall diameter deviations of the workpiece reveals the predominance of thermal effects in dry turning at the present workpiece geometry. The deformation of the tool accounts for the greatest inaccuracies. Calculated thermal expansions of the tool and the workpiece can be used in order to adapt the actual depth of cut accordingly. As a result, the accuracy of machining in dry turning is enhanced.

Acknowledgements

The authors would like to thank the German research foundation (DFG) for funding the project “Thermal effects when turning Al-MMC - experiments and simulations AU 185/26, STE 544/42” within the priority program SPP 1480.

References

[1] Klocke F, Eisenblätter G. Dry cutting. CIRP Ann Manuf Technol 1997;46/2:519–526.
[2] Sukaylo V, Kaldos A, Pieper HJ, Bana V, Sobczyk M. Numerical simulation of thermally induced workpiece deformation in turning when using various cutting fluid applications. J Mater Process Technol 2005;167/2-3:408-414.
[3] Moriwaki T, Horiuchi A, Okuda K. Effect of cutting heat on machining accuracy in ultra-precision diamond turning. CIRP Ann Manuf Technol 1990;39/1:81-84.
[4] Stephenson D, Barone M, Dargush G. Thermal expansion of the workpiece in turning. Trans ASME, J Eng Ind 1995;117/4:542–550.
[5] Klocke F, Lung D, Puls H. FEM-Modelling of the thermal workpiece deformation in dry turning. Procedia CIRP 2013; 8:239-244.
[6] Schindler S, Zimmermann M, Aurich JC, Steinmann P. Modeling deformations of the workpiece and removal of material when turning. Procedia CIRP 2013;8:39-44.
[7] Biermann D, Iovkov I. Modeling and simulation of heat input in deep-hole drilling with twist drills and MQL. Procedia CIRP 2013;8:87-92.
[8] Fleischer J, Pabst R, Kelemen S. Heat flow simulation for dry machining of power train castings. CIRP Ann Manuf Technol 2007;56/1:117–122.
[9] Denkena B, Schmidt A, Henjes J, Niederwestberg D, Niebuhr C. Modeling a Thermomechanical NC-Simulation. Procedia CIRP 2013;8:69-74.
[10] Zhou JM, Anderson M, Stahl JE. Identification of cutting errors in precision hard turning process. J Mater Process Technol 2004;153-154:746-750.
[11] Aurich JC, Zimmermann M, Schindler S, Steinmann P. Analysis of the machining accuracy when dry turning via experiments and finite element simulations. Prod Eng Res Devel 2014;8/1-2:41-50.
[12] Shaw MC. Metal cutting principles. New York: Oxford University Press; 2005.